Biochimica et Biophysica Acta, 687 (1982) 179–188
Elsevier Biomedical Press

BBA 71123

CALCIUM UPTAKE IN MASTOCYTOMA P-815 CELLS

MANABU NEGISHI, ATSUSHI ICHIKAWA and KENKICHI TOMITA *

Department of Health Chemistry, Faculty of Pharmaceutical Sciences, Kyoto University, Yoshida, Sakyo-ku, Kyoto 606 (Japan)

(Received September 15th, 1981)

Key words: Ca^{2+} uptake; Compartmentation; Cell cycle; (Mastocytoma cell)

Kinetic data of $^{45}Ca^{2+}$ exchange in exponentially growing mastocytoma P-815 cells at 37°C indicated the presence of at least two calcium compartments, fast and slowly exchangeable. The fast phase of calcium exchange at the cell surface had a rate constant of 36.1 min^{-1} and a compartment size of 8.27 nmol/10^6 cells, while the slow phase, the intracellular calcium exchange, showed a rate constant of 2.4 min^{-1} and a compartment size of 0.53 nmol/10^6 cells. The fast phase comprised two calcium binding sites of high and low affinities with dissociation constants of 0.59 and 4.88 mM, respectively, and binding maxima of 5.15 and 34.4 nmol/10^6 cells, respectively. The calcium uptake at both binding sites was inhibited by 80% on the addition of ruthenium red (0.4 mM) or lanthanum chloride (0.5 mM), but not by tetracaine (5 mM). The high-affinity site had two negative reaction enthalpy changes, $\Delta H^0 = -1.55$ (from 0 to 22°C) and -4.27 (from 22°C to 37°C) kcal·mol^{-1}, while the low-affinity site showed two positive reaction enthalpy changes, $\Delta H^0 = +6.53$ (below 22°C) and $+2.05$ (above 22°C) kcal·mol^{-1}, suggesting the effect of membrane fluidity on calcium binding. The slow phase of calcium exchange was also inhibited by ruthenium red and lanthanum chloride resulting in a decrease of the Hill's coefficient from 1.70 to 1.28 and 1.13, respectively, but was not affected by tetracaine. Calcium efflux from ^{45}Ca-loaded cells was also inhibited by ruthenium red and lanthanum chloride and was also temperature sensitive. The efflux rate constant was reduced by 80% and 100% at 20°C and 0°C, respectively. As calcium uptake fluctuated during the cell cycle of synchronous mastocytoma P-815 cells with a peak at the mid S phase and the lowest level during the late M phase, the compartment size of fast phase also fluctuated, being highest at the S phase and lowest at the M phase. In contrast, the compartment size of the slow phase was highest at the G_1 phase and lowest at the M phase. In parallel with these changes, the binding maximum of the high-affinity site was highest at the S phase and lowest at the M phase, while that of the low-affinity site fluctuated little throughout the cell cycle.

Introduction

Calcium appears to be an important growth regulator in a wide variety of cell types, and its extra- and intra-cellular concentrations, transport and intracellular sequestration systems seem to have significant influences on cellular proliferation and the cell division cycle [1–3]. However, cellular calcium metabolism is complicated because of the heterogeneity of cellular calcium pools. According to kinetic analyses of calcium fluxes in HeLa cells [4], rat pancreatic cells [5], mouse 3T3 cells [6] and rat heart cells [7], calcium is taken up into at least two kinetically defined compartments, fast and slowly exchanging. The fast phase of calcium uptake, which is removable with trypsin-EDTA [4,8], EGTA [6,9] or La^{3+} [7], presumably represents

* To whom correspondence should be addressed.

Abbreviations: EGTA, ethyleneglycol bis(β-aminoethyl ether)-*N*,*N*′-tetraacetic acid; Hepes, 4-(2-hydroxyethyl)-1-piperazineethanesulfonic acid.

Ca^{2+} binding to the cell surface, while the slow phase is not removable with these agents, representing Ca^{2+} uptake into the cell [4].

Apparently this calcium uptake fluctuates during the cell cycle, since a peak Ca^{2+}-level in the mid G_1 phase and its decline prior to entering the S phase have been reported in serum-stimulated 3T3 cells [6,10]. However, Ca^{2+} uptake of the fast and slow phases during the entire cell cycle has not been fully examined yet. In the present study, we have investigated several kinetic properties of Ca^{2+} uptake of these two phases in both exponentially and synchronously growing mastocytoma P-815 cells. A preliminary report of this work has appeared previously [11].

Materials and Methods

Cell culture

Mouse mastocytoma P-815 cells were maintained by suspension culture in Fischer-Sartorelli's medium supplemented with 5% fetal calf serum at 37°C in a 5% CO_2-containing humidified atmosphere as described previously [12]. Stock cultures were diluted every 1 or 2 days with the same fresh medium to maintain a cell density of $(0.8–4.5) \cdot 10^5$ cells/ml during exponential growth. Synchronization of mastocytoma cells at the beginning of the M phase by the colcemid block method or at the beginning of the S phase by the amethopterin block method was performed as described previously [13,14]. The cell number and cell volume were determined in a Coulter counter (Model Z, Coulter Electronics, Hialeah, FL, U.S.A.).

Calcium uptake assays

Mastocytoma P-815 cells in the exponential growth phase were harvested, washed three times with a medium containing 10 mM Hepes-NaOH buffer (pH 7.4), 137 mM NaCl, 4.15 mM KCl, 0.9 mM $CaCl_2$ and 1.05 mM $MgCl_2$ ('Hepes medium'), resuspended in the same medium ($5 \cdot 10^6$ cells/ml), and preincubated at 37°C for 10 min. The calcium uptake assay was initiated by the immediate addition of tracer $^{45}CaCl_2$ (final specific activity, 0.6 Ci/mol) to the cell suspension. After 5 s to 30 min of incubation at 37°C, aliquots (0.1 ml) were filtered using HAWP 0.45 μm Millipore filters. The filters were immediately rinsed three times with 2 ml of either 0.25 M sucrose (to remove unbound free calcium) or 0.9% NaCl containing 1 mM EGTA (to remove surface-bound calcium), dried, and placed in counting vials, dissolved in 2 ml of methyl cellosolve and ^{45}Ca-radioactivity counted in 10 ml of 0.5% 2,5-diphenyloxazole in toluene.

Kinetic analysis was performed using Borle's three-compartment closed system (extracellular, cell surface and intracellular) [4]. It was rather difficult, at early stages of reaction, to estimate calcium uptake of fast phase independently of that of slow phase. Therefore, after calcium uptake of both phases (of sucrose-washed cells) was plotted against time, kinetic parameters (half-time, rate constant, flux and compartment size) were calculated from semilogarithmic replots of ((maximal calcium uptake of both phases) − (calcium uptake of both phases at any given time)) (expressed as nmol calcium/10^6 cells) against time (usually for up to 2 min). Based on the preliminary experiments, the calcium uptake at 10 min at 37°C was taken as the maximal one, representing the sum of uptakes of both phases at equilibrium.

Calcium binding assay

Mastocytoma cells were harvested, washed three times with 'Ca^{2+}-free Hepes medium', preincubated at 37°C for 10 min in this Ca^{2+}-free medium, washed once and resuspended in the same medium ($5 \cdot 10^6$ cells/ml). After the addition of various concentrations (0.1 to 5 mM) of $^{45}CaCl_2$ (0.6 Ci/mol), each cell suspension was incubated at 37°C for 10 min, and maximal calcium uptake (sum of uptakes of both phases) was determined as described above. Calcium binding (to the cell surface) (= calcium uptake of fast phase) was then calculated by subtracting calcium uptake of slow phase from maximal calcium uptake. Since the compartment size of slow phase at equilibrium in the present study became practically constant (0.53 nmol/10^6 cells) at calcium concentrations above 50 μM (see Table I), this value was subtracted from the value of maximal calcium uptake. Binding data were plotted according to Scatchard [15], and analyzed by the hand estimation method of Rosenthal [16] to calculate the dissociation constant (K_d) and binding maximum (B_{max}).

Thermodynamic characteristics of calcium binding were examined with semilog plots of as-

sociation constants determined at different temperatures versus reciprocals of absolute temperatures ($1/T$). The standard enthalpy change (ΔH^0) of calcium binding was calculated from the van't Hoff equation: $d\ln K_a/dt = \Delta H^0/RT^2$ (R = gas constant). In a relatively narrow temperature range, this equation is integrated to $\ln K_a = \Delta H^0/T +$ constant, indicating a linear relationship between $\ln K_a$ and $1/T$. The standard free energy change (ΔG^0) and the standard entropy change (ΔS^0) of calcium binding were calculated from the equations: $\Delta G^0 = -RT\ln K_a$ and $\Delta G^0 = \Delta H^0 - T\Delta S^0$, respectively.

Calcium efflux assay

Mastocytoma cells were washed three times with 'Hepes medium' and preincubated ($5 \cdot 10^6$ cells/ml) at 37°C for 10 min in the same medium containing 0.9 mM $^{45}CaCl_2$ (0.6 Ci/mol). Ionophore A23187 (20 μg/ml, 40 μM) was then added to the cell suspension, and the mixture incubated at 37°C for 10 min. After centrifugation at 300 × g, the calcium-loaded cells were washed once with 'calcium-free Hepes medium' at 0°C. The washed cells retained a small amount of A23187 (0.2 nmol/10^6 cells, estimated spectrofluorometrically, activation at 267 nm and emission at 425 nm), which was not removed by repeated rinsing at 0°C. The cells were resuspended ($5 \cdot 10^6$ cells/ml) in the same medium, and incubated at 37°C. Aliquots (0.1ml) were withdrawn at various times to measure the amount of ^{45}Ca remaining in the cells as described above.

Materials

Hepes and EGTA were purchased from Nakarai Pure Chemicals (Kyoto, Japan). Tetracaine was obtained from Kyorin Seiyaku Co. (Tokyo, Japan). Procaine and lidocaine were purchased from Sigma Chemicals (St. Louis, MO, U.S.A.). Ionophore A23187 was obtained from Calbiochem-Behring Corp. (La Jolla, CA, U.S.A.). $^{45}CaCl_2$ (14 mCi/mg Ca) was purchased from New England Nuclear Corp. (Boston, MA, U.S.A.). Other chemicals of reagent grade were obtained commercially.

Results

Calcium uptake by mastocytoma P-815 cells

As observed in several other mammalian cells [4–7], Ca^{2+}-uptake into exponentially growing mastocytoma P-815 cells proceeded in two phases, an initial fast phase followed by a slow phase, and reached the maximum level within 2 min (Fig. 1). Rinsing the cells with EGTA resulted in a 95% reduction of the maximal calcium uptake. Kinetic parameters calculated from semilog replots (not shown) of the data in Fig. 1 are summarized in Table I. The rate constant and compartment size of the fast phase were about 15-fold greater than those of the slow phase. Based on the compartment size of slow phase (0.53 nmol/10^6 cells) and the cell volume ($0.803 \cdot 10^{-3}$ μl), the intracellular calcium concentration was estimated to be 0.66 mM.

Calcium uptake of fast phase

1. Calcium binding to mastocytoma P-815 cells. Preliminary investigations showed that the compartment size of the fast phase progressively increased with increasing concentrations of extracellular Ca^{2+} (from 0 to 5 mM), whereas that of the slow phase was relatively constant, increasing only in the calcium concentration range from 0 to 50 μM, and plateauing beyond that concentration (up to 5 mM) (data not shown). Based on these results, the calcium binding to the cell surface (fast phase) was examined at 10 min after the addition of 0.1 to 5 mM Ca^{2+} to the cell suspension. Since the

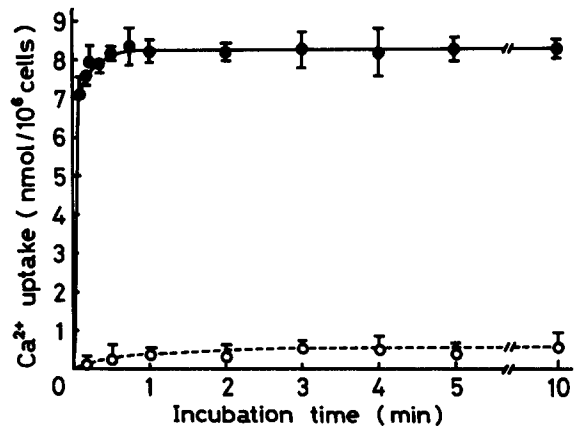

Fig. 1. Calcium uptake by mastocytoma P-815 cells. $^{45}Ca^{2+}$ uptake was assayed as described under Materials and Methods. After $^{45}Ca^{2+}$ uptake, the cells were washed with 0.25 M sucrose (●) or with saline containing 1 mM EGTA (○). Each point represents the mean ± S.E. of five determinations.

TABLE I

PARAMETERS OF Ca^{2+} UPTAKE INTO MASTOCYTOMA P-815 CELLS

Various kinetic parameters of the calcium compartments were obtained from semilog plots of the data in Fig. 1 as described under Materials and Methods. Each value represents the mean ±S.E. of five determinations.

Parameter	Fast phase	Slow phase
Half-time (min)	0.019± 0.002	0.29±0.03
Rate constant (min^{-1})	36.1 ± 2.4	2.40±0.31
Flux (nmol/10^6 cells per min)	299 ±23	1.30±0.12
Compartment size (nmol/10^6 cells)	8.27 ± 0.18	0.53±0.02

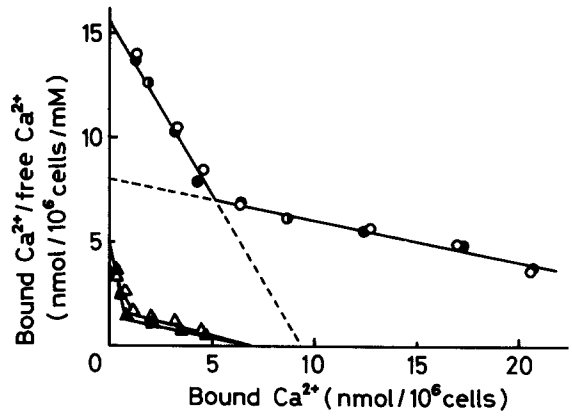

Fig. 2. Effect of ruthenium red, lanthanum chloride and tetracaine on Ca^{2+} binding. Cells were incubated for 10 min at 37°C in medium containing 0.1–5.0 mM Ca^{2+} without (●) or with 0.4 mM ruthenium red (▲), 0.5 mM lanthanum chloride (△) or 5 mM tetracaine (○). Then $^{45}Ca^{2+}$ uptake was measured, and the data were plotted according to Scatchard. Each point represents the mean of three determinations.

half time of of calcium uptake of the fast phase was 0.019 min (Table I), the calcium binding to the plasma membrane was assumed to reach equilibrium at 10 min. Scatchard plots (Fig. 2, ●) were biphasic, indicating the existence of at least two independent binding sites for calcium. From the extrapolated intercepts of linear segments of the plot, the high-affinity site with $K_d = 0.59$ mM was calculated to have a binding maximum of 5.15 nmol of calcium/10^6 cells. The low-affinity site with $K_d = 4.88$ mM had a binding maximum of 34.4 nmol of calcium/10^6 cells.

2. Effect of ruthenium red, tetracaine and lanthanum chloride. Ruthenium red, an inhibitor of calcium binding with glycoprotein, dose-dependently inhibited calcium uptake. The concentration required for half-maximal inhibition of calcium uptake in the presence of 0.9 mM Ca^{2+} was 0.2 mM. On the other hand, tetracaine, an inhibitor of calcium binding with phospholipid, did not affect calcium uptake at concentrations of up to 10 mM. Procaine and lidocaine also did not inhibit calcium uptake (data not shown). Scatchard plots showed that the binding maximums of both high- and low-affinity sites were reduced by more than 80% in the presence of 0.4 mM ruthenium red (Fig. 2, ▲), but they were not affected by 5 mM tetracaine (Fig. 2, ○) at all.

$LaCl_3$, a competitive inhibitor of Ca^{2+} binding, also dose-dependently inhibited the calcium uptake by mastocytoma cells. It caused half maximal inhibition of calcium uptake at 0.3 mM and almost complete inhibition at 2 mM in the presence of 0.9 mM Ca^{2+} (data not shown). Scatchard plots (Fig. 2, △) showed that the calcium binding maximums of both high- and low-affinity sites decreased by about 80% in the presence of 0.5 mM $LaCl_3$.

3. Effect of divalent cations. Among various divalent cations tested (Mg^{2+}, Sr^{2+}, Ba^{2+}, Mn^{2+}, Co^{2+}, Zn^{2+} and Ni^{2+}, from 0.01 to 1.0 mM) Zn^{2+} most strongly inhibited calcium uptake. Scatchard plots (not shown) showed that the dissociation constant and binding maximum of the high-affinity site were not affected by Zn^{2+} (Table II). In contrast, the dissociation constant of the low-affinity site increased, but the binding maximum was not affected in the presence of 0.1 or 1 mM Zn^{2+}. Zn^{2+} apparently competitively inhibited calcium binding to the low-affinity site.

4. Effect of temperature. The association constants (K_a) of Ca^{2+} binding to the two affinity sites in the temperature range from 0°C to 37°C were determined from Scatchard plots. With semilog plots of the K_a values versus reciprocals of absolute temperatures, two linear relationships were obtained for both high- and low-affinity sites, breaking at 22°C (Fig. 3). Using the van't Hoff equation, the reacting enthalpy changes (ΔH^0) were calculated to be −1.55 and −4.27 kcal·

TABLE II

EFFECT OF Zn^{2+} ON CALCIUM BINDING OF THE FAST PHASE

$^{45}Ca^{2+}$ uptake by mastocytoma P-815 cells was assayed under the standard conditions after the cells had been incubated with or without 0.1 mM or 1 mM $ZnCl_2$ for 10 min at 37°C. K_d and B_{max} were obtained from Scatchard plots of the data. Each value represents the mean ± S.E. of three determinations.

	High-affinity site		Low-affinity site	
	K_d (mM)	B_{max} (nmol/10^6 cells)	K_d (mM)	B_{max} (nmol/10^6 cells)
None	0.590±0.03	5.15±0.23	4.88±0.08	34.4±1.25
Zn^{2+} (0.1 mM)	0.596±0.04	4.90±0.31	7.39±0.01	34.8±2.01
Zn^{2+} (1.0 mM)	0.567±0.002	4.98±0.18	12.3±0.12	35.0±1.83

mol^{-1} for the high-affinity site, and +2.05 and +6.53 kcal · mol^{-1} for the low-affinity site. The standard free energy changes (ΔG^0) for calcium binding were calculated to be −0.42 and +0.959 kcal · mol^{-1} for the high- and low-affinity sites, respectively. Similarly, the standard entropy changes (ΔS^0) for calcium binding were calculated to be −12.9 and +3.66 cal T^{-1} · mol^{-1} for the high- and low-affinity sites, respectively.

Calcium uptake of slow phase

1. Effect of extracellular calcium concentration. As mentioned earlier, the compartment size of the slow phase decreased only when the extracellular Ca^{2+} concentration was below 50 μM. Plots of calcium uptake of the slow phase ((maximal uptake of both phases) − (uptake of fast phase at high and low affinity sites)) showed a sigmoidal function for calcium concentrations below 50 μM (data not shown). From the Hill plot of the experimental data, the Hill coefficient was found to be 1.70 (Fig. 4). Both ruthenium red and lanthanum chloride (0.5 mM) inhibited calcium uptake resulting in a decrease of the Hill coefficient to 1.28 and 1.13, respectively. On the other hand, tetracaine

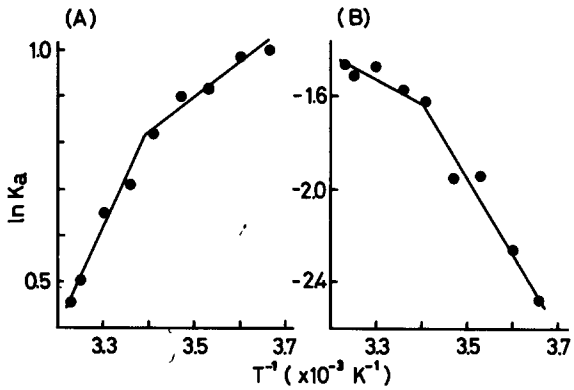

Fig. 3. Effect of temperature on Ca^{2+} binding of the fast phase. $^{45}Ca^{2+}$ uptake by the cells was measured at different temperatures from 0 to 37°C. K_a values were calculated as the reciprocals of K_d values obtained from the Scatchard plot of the uptake data. Each point represents the mean of three determinations.

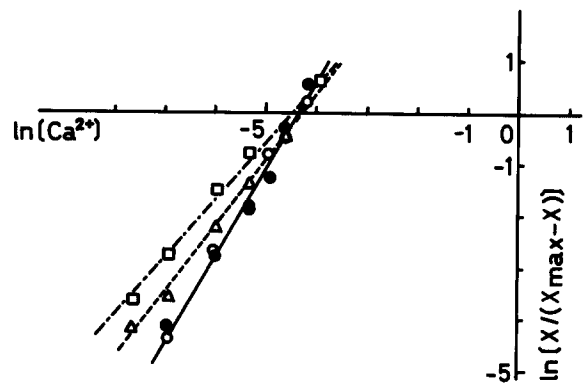

Fig. 4. Effect of ruthenium red, lanthanum chloride and tetracaine on calcium uptake of the slow phase. Cells were incubated in medium containing 2 to 50 μM Ca^{2+} without (●) or with 0.5 mM ruthenium red (△), 0.5 mM lanthanum chloride (□) or 5 mM tetracaine (○). The indicated values were obtained by subtracting the values (X) of Ca^{2+} binding to the high- and low-affinity sites calculated from the Scatchard plot from the maximal calcium uptake values (X_{max}). Each point represents the mean of three determinations.

(5 mM) did not affect the calcium uptake of the slow phase at all.

2. Effect of lanthanum chloride, ruthenium red and temperature on calcium efflux. A preliminary kinetic analysis by Borle's method indicated that the addition of calcium ionophore A23187 increased the compartment size of the slow phase by producing an additional compartment for that phase without affecting the compartment size of the fast phase (data not shown). A semilog plot of the calcium efflux from ^{45}Ca-loaded mastocytoma P-815 cells against time gave a straight line for about 10 min (Fig. 5). The calcium efflux rate constant was calculated to be 0.502 min^{-1}. This rate constant was reduced by approx. 50% on the addition of lanthanum chloride and ruthenium red (0.5 mM) (data not shown). The efflux rate constant also decreased by about 80% and 100% when the incubation temperatures were lowered from 37°C to 20°C, and 0°C, respectively (Fig. 5).

3. Non-involvement of Na^+-Ca^{2+} counter-transport. It is possible that the calcium efflux described above is mediated by the Na^+-Ca^{2+} countertransport system. However, replacement of NaCl in the incubation medium with KCl or choline chloride did not affect the calcium efflux (data not shown).

4. Calcium uptake during cell cycle. Calcium uptake by synchronized mastocytoma P-815 cells was at the lowest level during the late M and G_1 phases, then it increased gradually, reaching the highest level at the mid-S phase, and then decreased during the late S and G_2 phases (Fig. 6).

Kinetic analysis of Ca^{2+} uptake during the cell cycle was then performed selecting one representative point from each cell cycle phase: zero-time after removal of the colcemid block for the M phase, at 3 h for the G_1 phase, at 6 h for the S phase and at 9 h for the G_2 phase, respectively. As shown in Table III, rate constants did not significantly change throughout the cell cycle in both fast and slow phases. In contrast, the compartment size of the fast phase was highest at the S phase and lowest at the M phase, while the compartment size of the slow phase was highest at the G_1 phase and lowest at the M phase. These results coincided with the fluctuations of calcium uptake during the cell cycle.

Scatchard plots of calcium binding of the fast phase at the selected points of each cell cycle phase (not shown) showed that the binding maximum (B_{max}) of the low-affinity site fluctuated little during the cell cycle, but that of the high-

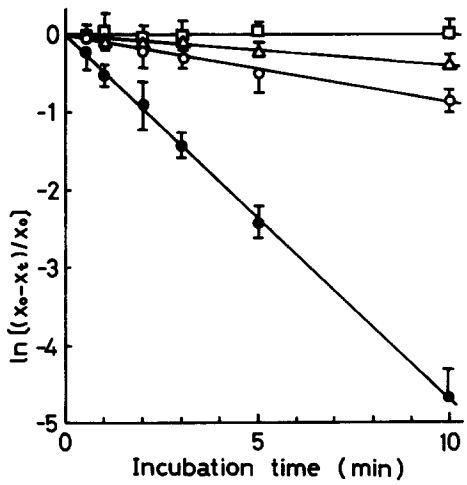

Fig. 5. Effect of temperature on calcium efflux. Cells loaded with $^{45}Ca^{2+}$ by treatment with A23187 were incubated in 'Ca^{2+}-free Hepes medium' at 37°C (●), 20°C (○), 10°C (△) or 0°C (□). About $5 \cdot 10^5$ cells were harvested at the given times and the remaining Ca^{2+} activity (X_t) (X_0 = the count at zero-time) was counted as described under Materials and Methods. Each point represents the mean ± S.E. of three determinations.

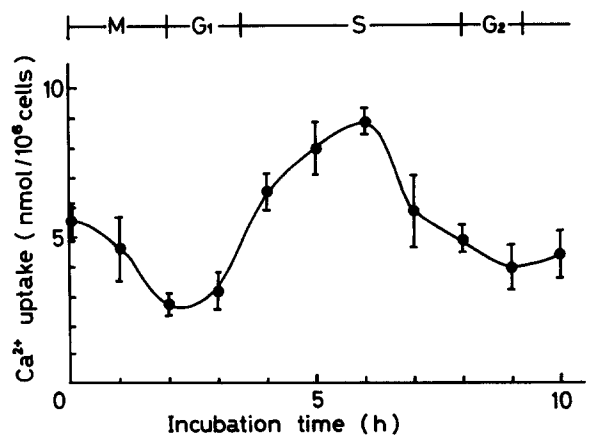

Fig. 6. Cell cycle dependency of calcium uptake. Cells ((2–3)·10^5 cells/ml, 100 ml) synchronized by the colcemid block method were incubated at 37°C. Aliquots (10 ml) of the cell suspension were withdrawn at different times after removal of the block, and assayed for calcium uptake. Each point represents the mean ± S.E. of three determinations.

TABLE III

CELL CYCLE DEPENDENCY OF Ca^{2+} UPTAKE PARAMETERS

Mastocytoma P-815 cells ((2–3)·10^5 cells/ml, 100 ml) were synchronized by the colcemid block method [13]. After removal of the block, aliquots of the synchronous cells were harvested at 0, 3, 6 and 9 h as representative of the M, G_1, S and G_2 phases, respectively. Parameters of calcium compartments were obtained as described in Table I.

Parameter	Cell cycle phase	Fast phase	Slow phase
Rate constant (min^{-1})	M	37.2 ± 3.8	2.32±0.43
	G_1	38.9 ± 4.1	2.45±0.29
	S	35.1 ± 5.9	2.11±0.32
	G_2	36.3 ± 2.3	2.25±0.18
Flux (nmol/10^6 cells per min)	M	205 ±18	0.67±0.08
	G_1	242 ±29	1.50±0.32
	S	309 ±21	1.19±0.23
	G_2	210 ±15	1.19±0.11
Compartment size (nmol/10^6 cells)	M	5.51± 0.56	0.29±0.02
	G_1	6.21± 0.39	0.67±0.05
	S	8.81± 0.41	0.56±0.02
	G_2	5.78± 0.24	0.53±0.07

affinity site significantly fluctuated, being lowest at the M phase and highest at the S phase (Table IV). The dissociation constant of the high affinity site also fluctuated, being lowest at the S phase and highest at the G_1 phase.

Hill plots of calcium uptake of the slow phase at the selected points of each cell cycle phase (not shown) showed that Hill coefficients did not significantly fluctuate, while the maximal uptake

TABLE V

CELL CYCLE DEPENDENCY OF Ca^{2+} UPTAKE OF THE SLOW PHASE

$^{45}Ca^{2+}$ uptake of the slow phase of synchronous mastocytoma P-815 cells at different phases of the cell cycle was analyzed using Hill's plots. Each value represents the mean±S.E. of three determinations.

Cell cycle phase	*n* value	Maximal uptake (nmol/10^6 cells)
M	1.61±0.05	0.333±0.081
G_1	1.67±0.04	0.625±0.105
S	1.63±0.04	0.531±0.088
G_2	1.62±0.08	0.526±0.096

fluctuated significantly during the cell cycle, being lowest at the M phase and highest at the G_1 phase (Table V).

In addition, EGTA added at the beginning of the S phase of mastocytoma P-815 cells synchronized by the amethopterin block method almost completely suppressed the subsequent cell division, while EGTA added at the beginning of the G_2 or M phase did not affect the normal cell cycle (data not shown).

Discussion

Data obtained by applying a mathematical model of Borle's three compartment closed system [4] indicated that in mastocytoma P-815 cells, as reported in several other mammalian cells [4–7], calcium was taken up into at least two kinetically

TABLE IV

CELL CYCLE DEPENDENCY OF Ca^{2+} UPTAKE OF THE FAST PHASE

Cells synchronized by the colcemid block method ((2–3)·10^5 cells/ml, 80 ml) were harvested at different phases of the cell cycle as in Table III, and used for Scatchard analysis of Ca^{2+} uptake. Each value represents the mean±S.E. of three determinations.

Cell cycle phase	High-affinity site		Low-affinity site	
	K_d (mM)	B_{max} (nmol/10^6 cells)	K_d (mM)	B_{max} (nmol/10^6 cells)
M	0.644±0.081	4.08±0.13	6.51±0.31	29.6±2.3
G_1	0.847±0.102	7.17±0.35	6.37±0.24	29.0±4.1
S	0.620±0.062	8.04±0.41	5.23±0.62	28.6±3.9
G_2	0.655±0.079	6.43±0.29	5.76±0.72	29.9±5.2

distinct compartments, fast and slowly exchanging (Table I).

The calcium uptake of the fast phase, representing calcium binding to the cell surface, was dependent on the extracellular calcium concentration and saturable. According to Scatchard plots (Fig. 2), the mastocytoma cell membrane appeared to have two types of binding sites with high and low affinities for calcium as observed for plasma membranes prepared from peritoneal mast cells [17], pancreatic islet cells [18] and hepatocytes [19] of rats. Since the calcium binding to both the sites was inhibited by lanthanum chloride [7,20] and ruthenium red [21], but not by tetracaine [22,23] (Fig. 2), the calcium pool of the fast phase was localized in the external plasma membrane and was probably glycoprotein and not phospholipid in nature. The high-affinity site appeared to be specific for Ca^{2+}, because the calcium binding to this site was not affected by Zn^{2+} (Table II), although Zn^{2+} and several other divalent cations inhibited the total calcium uptake. In contrast, Ca^{2+} binding to the low-affinity site was apparently competitively inhibited by Zn^{2+}. Furthermore, negative free energy changes indicated the thermodynamic stabilization of the high-affinity site on calcium binding. In contrast, Ca^{2+}-binding to the low-affinity site was more labile as indicated by the positive free-energy changes.

Abrupt shifts of reaction enthalpy changes occurred at about 22°C in both the sites (Fig. 3). We observed a similar temperature effect on prostaglandin E_1-induced cAMP accumulation in mastocytoma P-815 cells [24]. Refractoriness of mastocytoma cells to PGE_1 stimulation of cAMP accumulation developed within 1 min of incubation of the cells at 37°C, but disappeared immediately after lowering the temperature to below 23°C. Such shifts of the measured reaction enthalpy changes are often attributed to a thermotropic lipid phase transition, in which the lipid structure of the plasma membrane is transferred from the crystal phase to the liquid crystal phase at the critical temperature. These results suggest that both Ca^{2+} binding sites are influenced by the membrane fluidity. Similar phenomena were reported for several other membranous proteins such as adenylate cyclase [25,26], Ca^{2+}-ATPase [27], $(Na^+ + K^+)$-ATPase [28], concanavalin A receptors [29] and the alanine transport system [30].

The compartment size of the slow phase, regarded as the intracellular exchangeable Ca^{2+} pool, was very small as compared with that of the fast phase (Table I). The calcium uptake of the slow phase was also concentration-dependent, but only in the narrow range of calcium concentration up to 50 μM. The Hill plot of the slow phase of calcium uptake revealed the existence of a Ca^{2+} transport system which showed allosteric positive cooperativity with the Hill coefficient of 1.70 (Fig. 4). This Ca^{2+} transport system was also inhibited by ruthenium red and lanthanum chloride, but not by tetracaine.

$^{45}Ca^{2+}$ efflux from $^{45}Ca^{2+}$-loaded cells was also inhibited by ruthenium red and lanthanum chloride. Furthermore, the calcium efflux was temperature-sensitive, and the outflow rate constant decreased with decreasing incubation temperature, becoming zero at 0°C. Since ruthenium red is known to inhibit rat liver mitochondrial Ca^{2+} transport [31] and Ca^{2+}-activated membrane ATPase participating in Ca^{2+} transport in human red cell membrane [32], and also since the extracellular lanthanum is reported to block the active Ca^{2+} efflux and inhibit Ca^{2+}-ATPase in human red cells [33], these results suggest participation of Ca^{2+}-ATPase of the cell membrane in Ca^{2+} transport of mastocytoma cells. On the other hand, the Na^+-Ca^{2+} countertransport system, which is operative in rabbit cardiac membrane vesicles [34], dog red blood cells [35] and bovine heart plasma membrane [36], did not seem to take part in Ca^{2+} efflux in mastocytoma cells, because substitution of KCl or choline chloride for NaCl in the medium did not affect the Ca^{2+} efflux. However, elucidation of the role of Ca^{2+}-ATPase in the calcium transport in mastocytoma P-815 cells requires further investigation.

The discrepancy between the rate constant of the efflux (0.502 min^{-1}) and that of the slow phase (2.40 min^{-1}) (Table I) was probably due to the differences in the assay conditions. The calcium uptake of slow phase was assayed in steady state of influx and efflux of $^{45}Ca^{2+}$, while the efflux from $^{45}Ca^{2+}$-loaded cells was determined in non-steady state in which $^{45}Ca^{2+}$-influx was assumed to be negligible. The effect of a small amount of A23187 retained by the cells on the calcium efflux

was not clarified yet. These points also require further investigations.

Calcium has been implicated as a cell growth regulator, and the relationship between the cell cycle and calcium has been discussed for several types of cells such as mouse fibroblasts [6,10]. *Physalum polycephalum* [37] and *Tetrahymena* [38]. In synchronous mastocytoma P-815 cells, the peak of calcium uptake observed at the mid S phase (Fig. 6) correlated well with the highest level of compartment size of the fast phase (Table III) and also with the peak of binding maximum and the dissociation constant of the high-affinity site at the S phase (Table IV). Similarly, the lowest calcium uptake during the late M phase correlated with the lowest level of compartment size of the fast phase as well as that of the slow phase. In contrast, little significant changes in rate constant were observed for both fast and slow phases during the cell cycle. Furthermore, the complete inhibition of cell division by the addition of EGTA at the beginning of the S phase but not of the G_2 or M phase also suggested the important role of calcium uptake in the regulation of the cell cycle.

Fluctuation of membrane fluidity during the cell cycle has been reported in neuroblastoma cells [39,40] and chinese hamster ovarian cells [41]. Large modulations of the membrane permeabilities to K^+ and Na^+ during the cell cycle of mouse neuroblastoma cells also have been suggested to correlate with the cell cycle-dependent physicochemical membrane variations such as membrane fluidity and lateral mobility of lipids [42]. Therefore, fluctuations of compartment size, flux and membrane binding of calcium might be caused by perturbation of membrane fluidity during the cell cycle. Elucidation of this point is certainly required.

Acknowledgements

We are indebted to Yuko Ueha for excellent secretarial assistance. This work was supported in part by grants from The Ministry of Education, Science and Culture in Japan.

References

1 Whitfield, J.F., Boynton, A.L., MacManus, J.P., Rixon, R.H., Sikorska, M., Tsang, B., Walker, P.R. and Swierenga, S.H.H. (1980) Ann. N.Y. Acad. Sci. 339, 216–240
2 Swierenga, S.H.H., Whitfield, J.F., Boyton, A.L., MacManus, J.P., Rixon, R.H., Sikorska, M., Tsang, B.K. and Walker, P.R. (1980) Ann. N.Y. Acad. Sci. 341, 294–311
3 Berridge, M.J. (1975) in Advances in Cyclic Nucleotide Research (Greengard, P., Robinson, G.A., eds.), Vol. 6, pp. 1–98, Raven Press, New York
4 Borle, A.B. (1969) J. Gen. Physiol. 53, 43–56
5 Kondo, S. and Schulz, I. (1976) Biochim. Biophys. Acta 419, 76–92
6 Tupper, J.T., Del Rosso, M., Hazelton, B. and Zorgniotti, F. (1978) J. Cell. Physiol. 95, 71–84
7 Langer, G.A. and Frank, J.S. (1972) J. Cell Biol. 54, 441–455
8 Borle, A.B. (1968) J. Cell Biol. 36, 567–581
9 Tupper, J.T. and Zorgniotti, F. (1977) J. Cell Biol. 75, 12–22
10 Paul, D. and Ristow, H.J. (1979) J. Cell. Physiol. 98, 31–40
11 Tomita, K., Negishi, M. and Ichikawa, A. (1980) Fed. Proc. 39, 2155
12 Ichikawa, A., Esumi, K., Takagi, M., Yatsunami, K., Negishi, M., Yokoyama, K. and Tomita, K. (1980) J. Pharmaco-bio. Dyn. 3, 123–135
13 Ichikawa, A., Negishi, M., Tomita, K. and Ikegami, S. (1980) Jap. J. Pharmacol. 30, 301–308
14 Negishi, M., Ichikawa, A., Oshio, N., Yatsunami, K. and Tomita, K. (1982) Biochem. Pharmac. 31, 173–179
15 Scatchard, G. (1949) Ann. N.Y. Acad. Sci. 51, 660
16 Rosenthal, H.E. (1967) Anal. Biochem. 20, 525–532
17 Tolone, G., Bonasera, L., Vitale, F. and Pontieri, G.M. (1980) Int. Arch. Allergy Appl. Immunol. 63, 236–239
18 Naber, S.P., McDonald, J.M., Jarett, L., McDaniel, M.L., Ludvigsen, C.W. and Lacy, P.E. (1980) Diabetologia 19, 439–444
19 Shaltz, J. and Marinetti, G.V. (1972) Biochim. Biophys. Acta 290, 70–83
20 Weiss, G.B. (1974) Annu. Rev. Pharmacol. 14, 343–354
21 Kamino, K., Ogawa, M., Uyesaka, N. and Inouye, A. (1976) J. Membrane Biol. 26, 345–356
22 Feinstein, M.B. (1964) J. Gen. Physiol. 48, 357–373
23 Lüllmann, H., Plösch, H. and Ziegler, A. (1980) Biochem. Pharmac. 29, 2969–2974
24 Yatsunami, K., Ichikawa, A. and Tomita, K. (1981) Biochem. Pharmac. 30, 1325–1332
25 Rene, E., Pecker, F., Stengel, D. and Hanoune, J. (1978) J. Biol. Chem. 253, 838–841
26 Pliego, J.A. and Rubalcava, B. (1978) Biochem. Biophys. Res. Commun. 80, 609–615
27 Madden, T.D., Chapman, D. and Quinn, P.J. (1979) Nature 279, 538–540
28 Giraud, F., Claret, M., Bruckdorfer, K.R. and Chailley, B. (1981) Biochim. Biophys. Acta 647, 249–258
29 B.-Bassat, H., Polliak, A., Rosenbaum, S.M., Naparstek, E., Shouval, D. and Inbar, M. (1977) Cancer Res. 37, 1307–1312
30 Ryan, J. and Simoni, D. (1980) Biochim. Biophys. Acta 598, 606–615
31 Moore, C.L. (1971) Biochem. Biophys. Res. Commun. 42, 298–305
32 Watson, E., Vincenzi, R.R. and Davis, P.W. (1971) Biochim. Biophys. Acta 249, 606–610

33 Szász, I., Sarkadi, B., Schubert, A. and Gardos, G. (1978) Biochim. Biophys. Acta 512, 331–340
34 Reeves, J.P. and Sutko, J.L. (1979) Proc. Natl. Acad. Sci. U.S.A. 76, 590–594
35 Parker, J.C. (1978) J. Gen. Physiol. 71, 1–17
36 Miyamoto, H. and Racker, E. (1980) J.Biol. Chem. 255, 2656–2658
37 Holmes, R.P. and Stewart, P.R. (1977) Nature 269, 592–594
38 Walker, G.M. and Zeuthen, E. (1980) Exp. Cell Res. 127, 487–490
39 De Laat, S.W., Van der Saag, P.T. and Shinitzky, M. (1977) Proc. Natl. Acad. Sci. U.S.A. 74, 4458–4461
40 De Laat, S.W., Van der Saag, P.T., Elson, E.L. and Schlessinger, J. (1980) Proc. Natl. Acad. Sci. U.S.A. 77, 1526–1528
41 Lai, C.-S., Hopwood, L.E. and Swartz, H.M. (1980) Biochim. Biophys. Acta 602, 117–126
42 Boonstra, J., Mummery, C.L., Tertoolen, L.G.J., Van der Saag, P.T. and De Laat, S.W. (1981) J. Cell. Physiol. 107, 1–9